

# Finite Element Analysis and Experimental Investigation on the Conventional and Vibration Assisted Drilling

Mehdi Nosouhi<sup>1,2</sup>, Reza Nosouhi<sup>1,2\*</sup>, Hossein Paktinat<sup>2</sup>, Saeid Amini<sup>3</sup>

<sup>1</sup>Modern Manufacturing Technologies Research Center, Najafabad Branch, Islamic Azad University, Najafabad, Iran

<sup>2</sup>Department of Mechanical Engineering, Najafabad Branch, Islamic Azad University, Najafabad, Iran

<sup>3</sup>Manufacturing Department, Faculty of Mechanical Engineering, University of Kashan, Kashan, Iran

\*Email of Corresponding Author: rezaanosouhi@gmail.com

Received: September 9, 2017; Accepted: January 31, 2018

## Abstract

In this research, finite element analysis of the conventional drilling and vibration assisted drilling is carried out. The ABAQUS software is employed for FE analysis. The Johnson-Cook models for both plastic deformation and damage are employed for FE simulation. The results of the FE analysis are then verified with experimental results in both conventional and vibration assisted drilling on Al 7075 with HSS drill in terms of the drilling axial force and torsional torque. There is a good agreement between the experimental results and the FE simulation results. The results also show that the drilling axial force and torsional torque are reduced in vibration assisted drilling in comparison with that in conventional drilling process. The surface roughness of the holes is also studied in conventional drilling and vibration assisted drilling. The results showed that the surface roughness is excelled in vibration assisted machining in comparison with that in conventional drilling.

## Keywords

FE Analysis, Vibration Assisted Drilling, Conventional Drilling, Experiment, Al7075

## 1. Introduction

The vibration assisted drilling is a drilling process in which a vibrational movement (usually with ultrasonic frequencies) is superimposed with the drilling movement (usually in the longitudinal direction). Therefore the continuous contact between the workpiece and the drill is turned into an intermittent contact. The reduction in the axial force and torsional torque along with reduction in the generated heat in the cutting zone in comparison with the conventional drilling process are the advantages of using this process. The process is therefore employed for drilling some hard-to-cut materials.

There are some research works available in literature. Wang et al. presented a model for prediction of the axial force and torsional torque in vibration assisted drilling. The presented model is the result of the vibration analysis [1]. Isbilir and Ghassemieh [2] numerically simulated the conventional drilling process. Guibert et al. investigated on the effect of the drill geometry on the drilling force [3]. They suggested an optimized geometry for drills. Lauderbaugh performed a statistical analysis on simulation and experimental results and derived the optimized parameters in drilling [4]. Guibert et al. studied the dynamic behavior of the drill in vibration assisted drilling [5]. They also validated the results with experiments. They claimed that the vibration assisted drilling

process can be employed for drilling the deep holes without coolant. Vijayaraghavan and Dornfeld worked on the modeling of the drill for FE analysis [6]. Guo and Dornfeld numerically studied the chip formation in conventional drilling process of steel 304 [7]. Yen et al. [8] investigated on the size of the hole produced in vibration assisted drilling and showed that the hole size in vibration assisted drilling was slightly smaller than that in conventional drilling. Babitsky et al. [9] showed that the drilling force was significantly reduced in vibration assisted drilling process. Neugebauer and Stoll [10] showed that the main reason of the force reduction in vibration assisted drilling was the reduction of the chip sizes.

In this research, finite element analysis of conventional and vibration assisted drilling of Al 7075 T6 was carried out. ABAQUS explicit was employed for FE analysis. The results are then verified with experimental results.

## 2. Materials and Methods: FE Analysis of the Processes

The ABAQUS explicit solver was employed to simulate the drilling process. The geometry of the drill was firstly generated in CATIA software. Then the model was imported in ABAQUS software. The drill was defined as a discrete rigid body and the workpiece defined as a deformable geometry. The V-bottom hole was primarily generated in the workpiece so that the entire edge of the drill would be engaged with the workpiece from the beginning. The Johnson-Cook model was employed both for plastic deformation and for damage. The material model is presented as follows:

$$\sigma_y = [A + B\varepsilon_p^n] \left[ 1 + C \ln\left(\frac{\dot{\varepsilon}_p}{\dot{\varepsilon}_{p0}}\right) \right] \left( 1 - \left( \frac{T - T_0}{T_m - T_0} \right)^m \right) \quad (1)$$

In which  $\sigma_y$  is the material flow stress,  $\varepsilon_p$  is the equivalent plastic strain,  $T_m$  is the melting temperature of the material,  $T$  is the material temperature,  $T_0$  is the reference temperature,  $\dot{\varepsilon}_p$  is the plastic strain rate,  $\dot{\varepsilon}_{p0}$  is the effective plastic strain rate of the quasi static test and  $A$ ,  $B$ ,  $C$ ,  $m$ ,  $n$  are the material constants.

The Johnson-Cook damage model was also employed for modeling of the burr formation. The model is presented in Equation 2. In this model, the damage occurs whenever the parameter  $D$  exceeds 1.

$$D = \sum \frac{\Delta\bar{\varepsilon}^{pl}}{\bar{\varepsilon}_f^{pl}} \quad (2)$$

In which  $\Delta\bar{\varepsilon}^{pl}$  is the plastic tension increase and  $\bar{\varepsilon}_f^{pl}$  is the tension needed for damage and is calculated from Equation 3:

$$\bar{\varepsilon}_f^{pl} = \left[ d_1 + d_2 \exp d_3 \left( \frac{p}{q} \right) \right] \left[ 1 + d_4 \ln \frac{\varepsilon_{pl}}{\dot{\varepsilon}_0} \right] \left( 1 + d_5 \frac{T - T_0}{T_m - T_0} \right) \quad (3)$$

In which  $p$  is the compressive stress,  $q$  is the von-misses stress, The Johnson-Cook damage parameters are also presented in Table 1:

Table1. Johnson-Cook material constants for plastic deformation and damage

Parameter	Value
A (MPa)	546
B (MPa)	674
$n$	0.72
$c$	0.059
$m$	1.56
$T_m$ (°C)	580
Initial failure strain, $d_1$	-0.068
Exponential factor, $d_2$	0.451
Triaxiality factor, $d_3$	-0.952
Strain rate factor, $d_4$	0.036
Temperature factor, $d_5$	0.697

To reduce the simulation time, only a section of the drill which was engaged with the workpiece was modeled. To ensure the validity of the analysis, mesh study was carried out and the convergence of the results was approved.

The simulated drilling process is depicted in Figure 1.

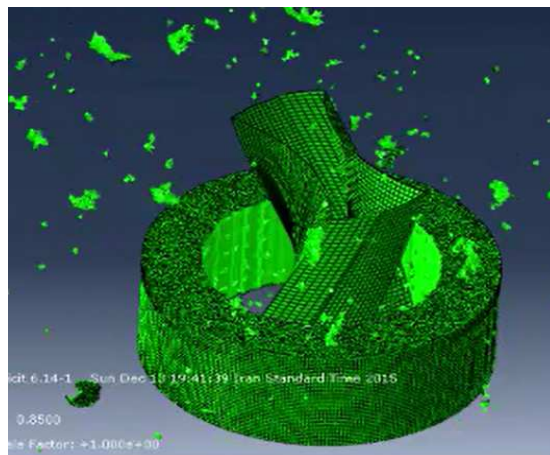


Figure1. The simulated drilling process

The simulation was performed both for conventional drilling and vibration assisted drilling. The simulation here is performed with a discrete rigid drill bit and a deformable workpiece. The Johnson-cook deformation and damage material models have been employed for simulation. In Figure 1 it is depicted that how the drilling chips are formed and the hole is fabricated.

### 3. Experimental Tests

A vibration assisted drilling test setup was used for experimental tests. The following modules were included in the test setup:

- The milling machine (Deckle FP4)
- Dynamometer (Kistler 9250B)

- Ultrasonic generator (MPI)
- Transducer and horn
- Gap sensor for measurement of the vibration amplitude (AEC PU-02)
- The oscilloscope and signal generator
- Surface roughness measurement apparatus (MahrPerthometer M2)
- HSS drill (diameter =5 mm)
- 

The test setup is illustrated in Figure 2.



Figure2. The test setup

The test setup elements are schematically illustrated in Figure 3.

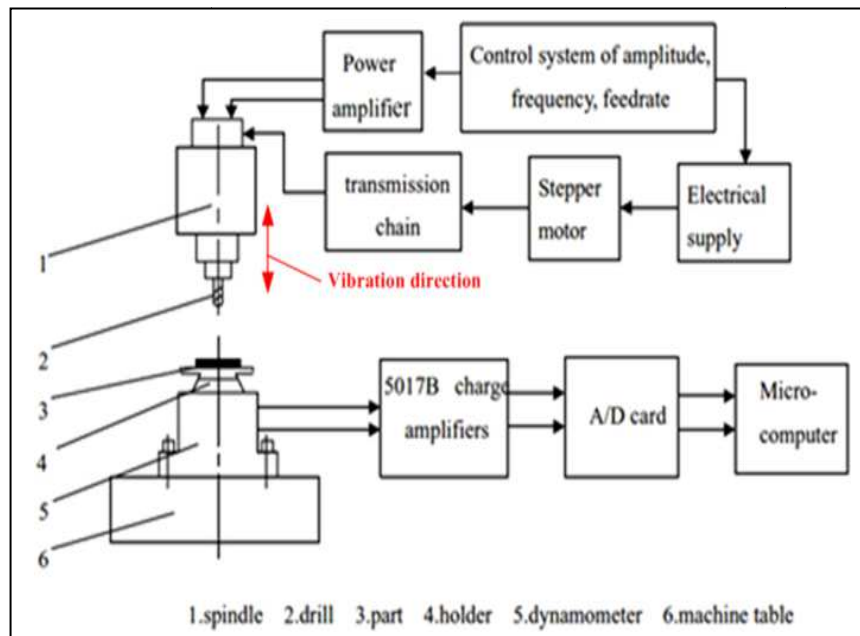


Figure3. Schematic illustration of the test setup

### 3.1 The Experimental Parameters

The drill was assembled on the horn and the transducer, all of which were mounted on the milling machine spindle. The transducer along with the generator produced the ultrasonic vibration.

The tests were performed under different conditions. The test parameters are presented in Table 2.

Table2. The test parameters

Parameter	Value	Unit
Vibration Frequency	19.8	kHz
Vibration amplitude	8	$\mu\text{m}$
Feed rate	0.08	mm/rev
	0.11	
	0.14	
	0.2	
Cutting speed	250	rpm
	350	
	500	
	700	
	1000	

After adjustments on the feed rate and drilling speed, the drilling tests were started with assistance of the vibration. After passing the half of the hole final depth, the generator was switched off and the rest of the hole was generated without the assistance of vibration. Since the tool wear increases the cutting forces and vibration, a new drill was used for each of the tests.

## 4. Results and Discussion

### 4.1 The Force Results

The measured forces in the experimental tests are presented as follows:

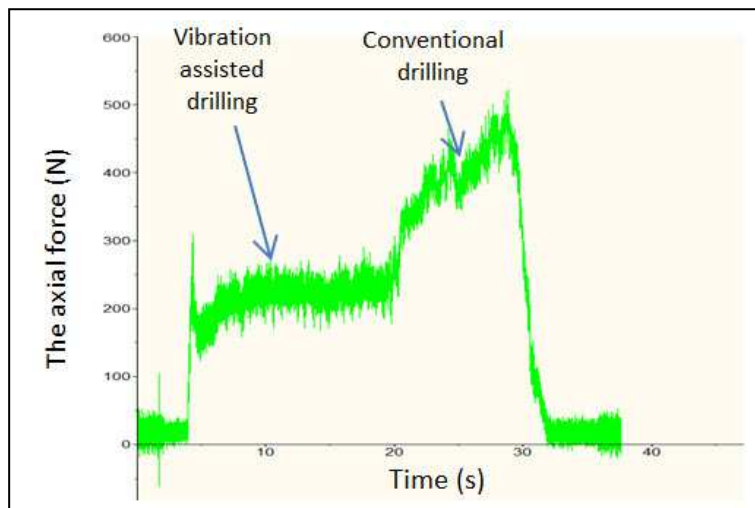


Figure4. The measured forces

As it can be seen in Figure 4, the force was reduced as a result of vibration assisted drilling. There are some reasons for this observation. One of the reasons is the reduction of the chip sizes. Also, the sticking of the drill to the hole's walls reduces as a result of the vibration.

#### 4.2 Comparison between the Simulation and Experimental Results

To verify the simulation results, the force achieved from the simulation was compared with that from experiment. The results are depicted in Figure 5.

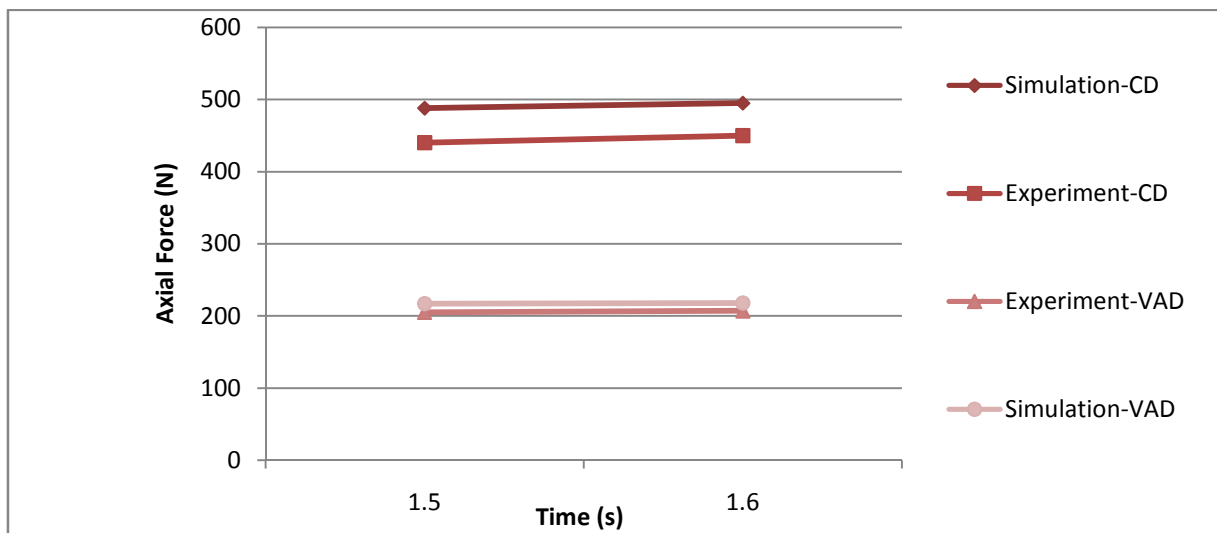


Figure 5. The comparison between the axial forces achieved from simulation and experiment

The simulation results show good agreement with experimental results. The amount of the normalized error between the numerical and experimental results in vibration assisted drilling is 5 percent, and is 9 percent in conventional drilling.

A comparison was also made between the forces achieved from simulation and experiment. The results are depicted in Figure 6.

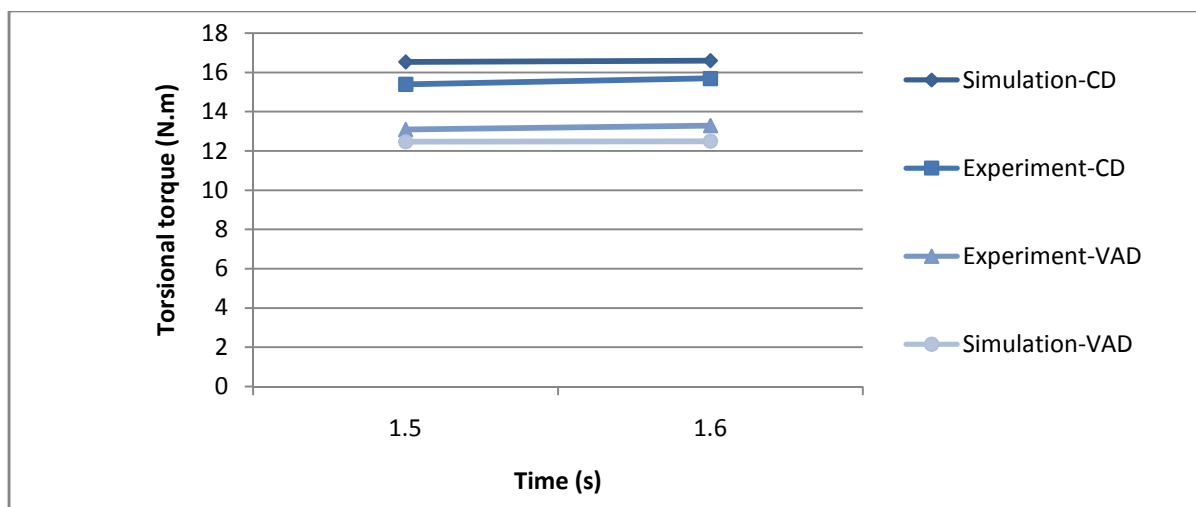


Figure 6. The comparison between the torsional torques achieved from simulation and experiment

As it can be seen in Figure 6, there is good agreement between the simulation and experimental results. The amount of the normalized error in vibration assisted drilling is 5 percent, which is about 6 percent in conventional drilling.

#### 4.3 The Effects of the Feed Rate and Cutting Speed on the Results

The effects of the cutting speed on the torsional torque and axial force are presented in Figures 7 and 8 respectively.

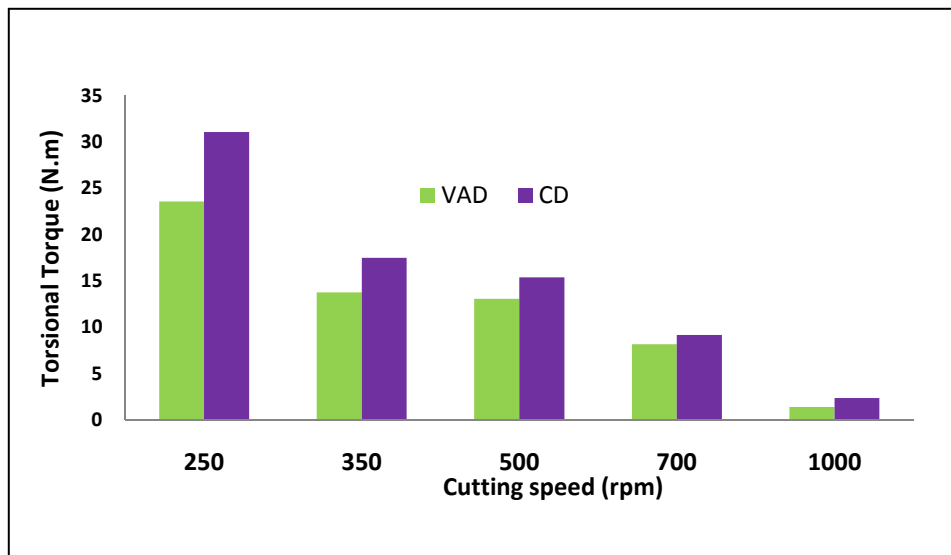


Figure7. The effect of the cutting speed on the torsional torque

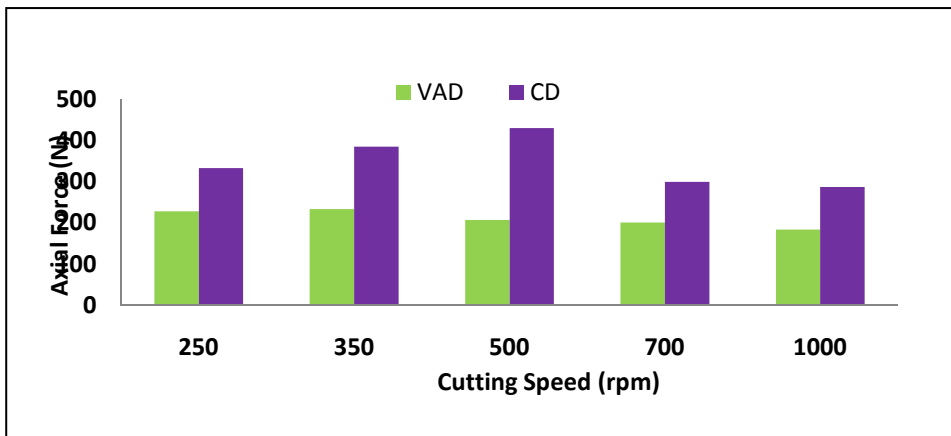


Figure8. The effect of the cutting speed on the axial force

Figure 7 shows that the torsional torque decreases as a result of increase in the cutting speed. This is mainly because of the thermal softening that occurs as a result of increase in the cutting speed and consequently, the cutting zone temperature. The same trend could be observed about the axial force. The peak point that exists in the force diagram is because of the built-up edge phenomenon which increases the force.

The effects of the feed rate on the torsional torque and axial force are presented in Figures 9 and 10 respectively.

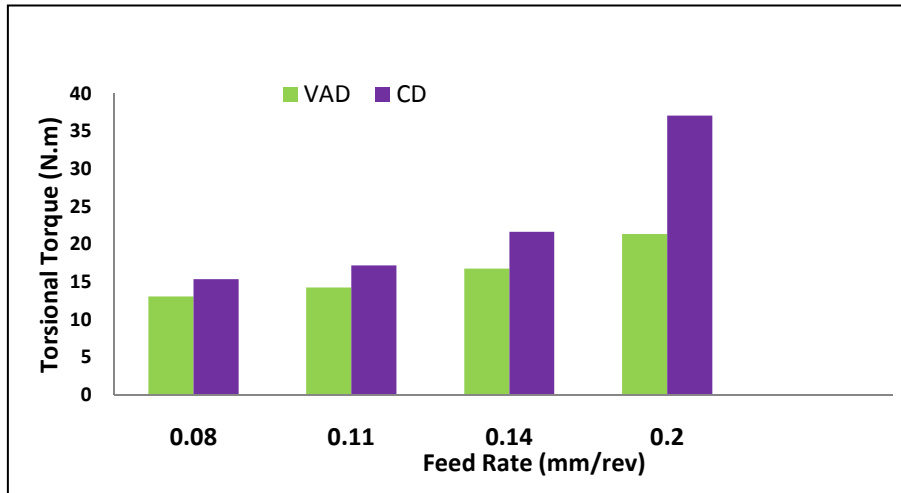


Figure9. The effect of the feed rate on the torsional torque

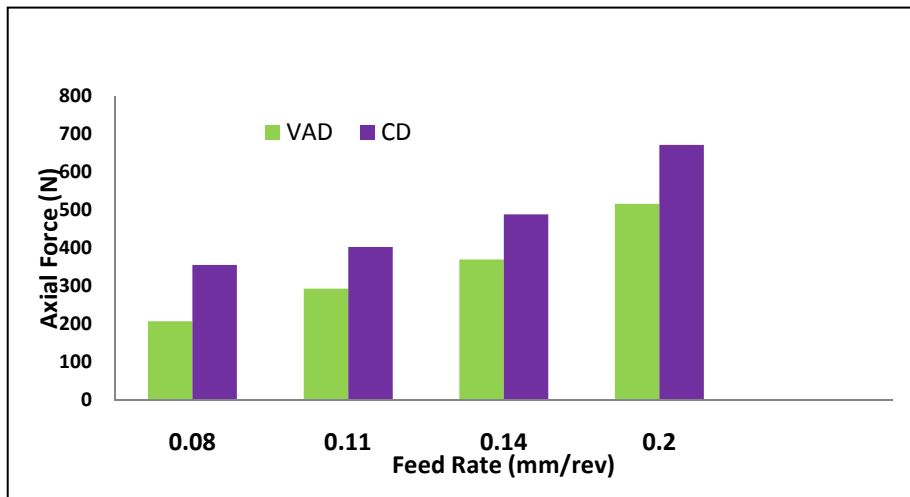


Figure10. The effect of the feed rate on the axial force

As it can be seen in Figures 9 and 10, the amounts of both torsional torque and axial force increase as the feed rate increases. This is mainly because of the increase in the uncut chip thickness as a result of increase in the feed rate.

#### 4.4 The Effect of the Cutting Speed and Feed Rate on the Surface Roughness

In vibration assisted drilling process, the sticking between the drill and the hole surface is less than that in conventional drilling. Furthermore, in vibration assisted drilling the chips are not continuous and the contact between the chips and the hole's wall is less. Therefore the hole's surface roughness in vibration assisted drilling is less than that in conventional drilling. The results of the surface roughness are presented in Figure 11.

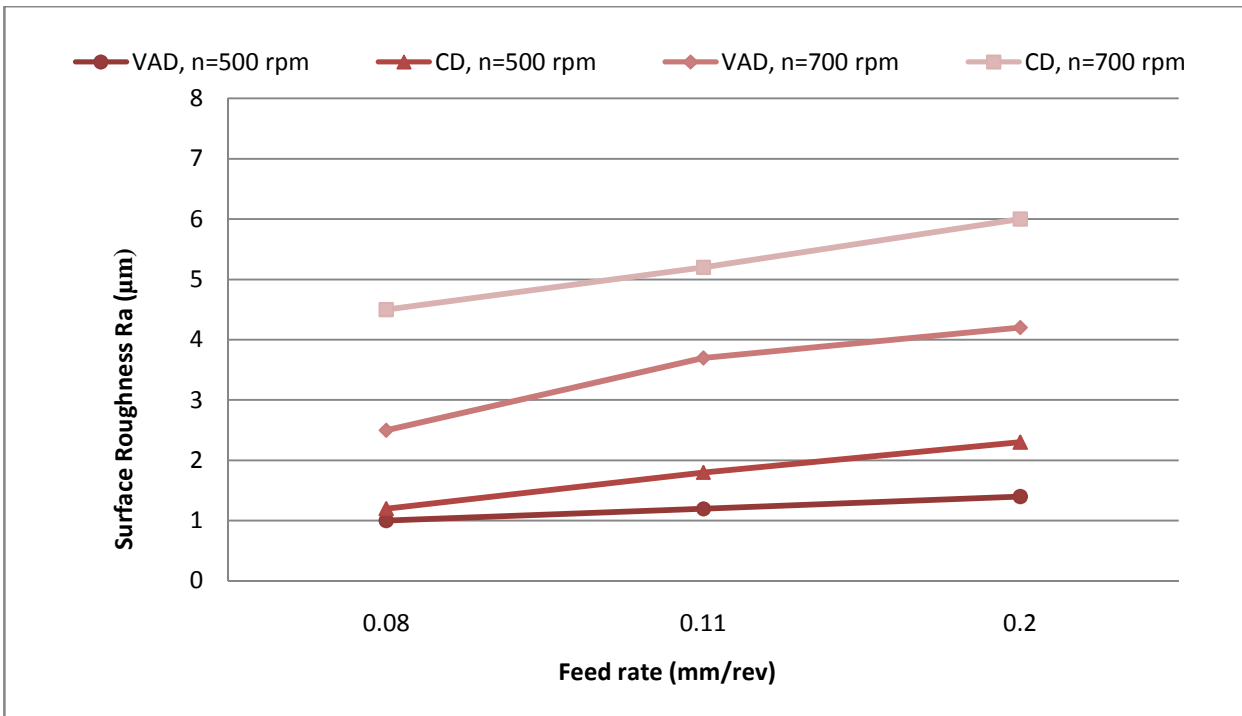


Figure11. The effect of the feed rate and cutting speed on the surface roughness

The surface roughness was increased as the feed rate was increased. The reason is that the increase in the feed rate would increase the height of the tool marks on the machined surface. Also, the surface roughness in vibration assisted drilling was less than that in conventional drilling. A cross section of the workpiece in both machining conditions is presented in Figure 12. As it can be seen, the surface in vibration assisted drilling was smoother than that in conventional drilling.



Figure12. The cross section of the workpiece a) in conventional drilling and b) in vibration assisted drilling

#### 4.5 The Produced Chips

One of the most important factors in machining is the chip shape and type. The continuous chips are causing so many troubles in machining as they may harm the operator and may damage the tool or workpiece. Many researchers are nowadays working on the strategies so that the chips break while machining and the formation of continuous chips could be avoided. In vibration assisted drilling process, because of the intermittent nature of the process, the chips break automatically even in drilling of the soft materials. This is one of the main advantages of this process. The shape of the chips in both conventional drilling and vibration assisted drilling is depicted in Figure 13.



Figure13. The chips in a) conventional drilling and b) vibration assisted drilling

As it can be seen in Figure 13, the chips which were produced in vibration assisted drilling were discontinuous and segmental, while the produced chips in conventional drilling were continuous.

## 5. Conclusion

The FE simulation of the conventional and vibration assisted drilling was carried out in this research. The ABAQUS software was employed for FE simulation, and the results were validated with the experimental results afterward. A set of experiments was also performed on both conventional and vibration assisted drilling processes in terms of the axial force and torsional torque and their dependency to the feed rate and cutting speed, surface roughness and produced chips' shape. The main results are listed below:

- There was good agreement between the simulation and experimental results, which shows the validity of the FE simulation.
- The axial force and torsional torque increased as the feed rate increased, as it was expected.
- The axial force and torsional torque decreased as the cutting speed was increased, which was mainly because of the thermal softening.
- The surface roughness in vibration assisted drilling was excelled in comparison with conventional drilling process.
- The produced chips in vibration assisted drilling process were discontinuous and segmental, while the chips produced in conventional drilling were continuous. This phenomenon was because of the intermittent nature of the vibration assisted drilling process.

## 6. References

- [1] Wang, L-P., Wang, L-J., He, Y-H., Yang, Z-J. 1998. Prediction and Computer Simulation of Dynamic Thrust and Torque in Vibration Drilling. *Proceedings of the Institution of Mechanical Engineers, Part B: Journal of Engineering Manufacture*. 212(6): 489-497.
- [2] Isbilir, O., Ghassemieh, E. 2011. Finite Element Analysis of Drilling of Titanium Alloy. *Procedia Engineering*. 10: 1877-1882.
- [3] Guibert, N., Paris, H., Rech, J. and Claudin, C. 2009. Identification of Thrust Force Models for Vibratory Drilling. *International Journal of Machine Tools & Manufacture*. 49(9): 730–738.
- [4] Lauderbaugh, L. K. 2009. Analysis of the Effects of Process Parameters on Exit Burrs in Drilling Using a Combined Simulation and Experimental Approach. *Journal of materials processing technology*. 209(4): 1909–1919.

- [5] Guibert, N., Paris, H. and Roch, J. 2008. A Numerical Simulator to Predict the Dynamical Behavior of the Self-Vibratory Drilling Head. *International Journal of Machine Tools & Manufacture*.48(6): 644–655.
- [6] Vijayaraghavan, A. and Dornfeld, D. A. 2007. Automated Drill Modeling for Drilling Process Simulation. *Journal of Computing and Information Science in Engineering*. 7(3): 276-282.
- [7] Guo, Y.B. and Dornfeld, D.A. 1999. Finite Element Modeling of Burr Formation Process in Drilling 304 Stainless Steel. *Journal of Manufacturing Science and Engineering*. 122(4): 612-619.
- [8] Yen, Y-C., Jain, A. and Altan, T. 2004. A Finite Element Analysis of Orthogonal Machining Using Different Tool Edgegeometries. *Journal of Materials Processing Technology*. 146(1): 72–81.
- [9] Babitsky, V.I., Astashev, V.K. and Meadows, A. 2007. Vibration Excitation and Energy Transfer During Ultrasonically Assisted Drilling. *Journal of Sound and Vibration*. 308(3-5): 805–814.
- [10] Neugebauer,R. and Stoll, A. 2004. Ultrasonic Application in Drilling. *Journal of Materials Processing Technology*. 149(1-3): 633-639.